Digital Frequency Multipliers Using Multisection Two-Strip Coupled Line

IWATA SAKAGAMI, NOBUSHIRO MIKI, MEMBER, IEEE, NOBUO NAGAI, MEMBER, IEEE, AND KOZO HATORI, SENIOR MEMBER, IEEE

Abstract—**This paper describes new networks which acts as digital frequency multipliers such as doubler, tripler, and so on for input clock frequency. The networks consist of cascaded sections of uniform lossless commensurate coupled-transmission-lines and three resistors of Π-structure, and the proposed multipliers are quite new in the sense of being built without using active or nonlinear circuit elements. The theoretical and experimental results for a coupled-line digital frequency doubler are compared and found to be in good agreement.**

I. Introduction

A CONSTANT-RESISTANCE distributed coupled-line network consisting of cascaded sections of uniform lossless commensurate two-strip coupled transmission line and three resistors of Π-structure, which was primarily reported in microwave region as an amplitude equalizer [1], is treated and the time domain behaviors of the coupled-line network are discussed.

Generally speaking, the analysis and synthesis of the distributed line or coupled-line network have received much attention in the frequency domain [1]–[5], but relatively little in the time domain [6]–[8]. However, the time domain analysis and its application have become increasingly important with the advent of fast rise-time pulse techniques, high-speed microminiature circuits, and the computer industry [9]. The output voltage waveform for an arbitrary input voltage waveform can be readily obtained from the impulse response of the network under consideration and the convolution theorem. Therefore, the Fourier-transform, Laplace-transform, and z-transform are well-known techniques to derive the impulse response from the transfer function of the distributed line or coupled-line network [7], [10]. Thus, we can investigate the time domain properties of these networks originated in microwave frequency range.

Here, by using z-transform and signal flow graph techniques, it is clarified that digital frequency multipliers such as doubler, tripler, and so on for input clock frequency can be constructed from the constant-resistance coupled-line networks of multisection without using active or nonlinear circuit elements. Several investigators [11]–[13] have reported the results on the frequency multipliers, but all of these contain active elements as the constituents. The proposed digital frequency multipliers are quite new in the sense of being built with only passive elements and also of preparing equiamplitude pulses according to the principle of superposition every time interval 2τ, where $2\tau=2l/v$: l is the length of coupled-line of one section and v is the speed of light in the medium. The equiamplitude pulses with period 2τ may be composed of the returning wave superposed at the output port. Therefore, on designing the proposed digital frequency multipliers, the time interval 2τ or the coupled-line length l must be chosen so as to become one mth ($m=2,3,\cdots$) as long as the period of input clock frequency. The experimental results showing an excellent agreement with theory are presented for the digital frequency doubler.

Manuscript received June 25, 1980; revised September 16, 1980.

The authors are with the Research Institute of Applied Electricity, Hokkaido University, Sapporo, 060 Japan.

II. Signal Flow Graph for Constant-Resistance Coupled-Line Network

The network under consideration is shown in Fig. 1. The symmetry of this network allows the use of the method of even- and odd-mode excitations at the two ports A_1 and A_2. The equivalent circuits of both even and odd modes are shown in Fig. 2. The y_{ei} and y_{oi} ($j=1,2,\cdots,n$) are the even- and odd-mode normalized characteristic admittances. The r_{ej} and t_{ej} ($i=1,2,\cdots,n+1$) are the reflection and transmission coefficients of the even mode, and r_{oj} and t_{oj} are also those of odd mode. The g_1 and g_2 are normalized conductances. These y_{ei}, y_{oi}, g_1, and g_2 have following relations:

$$y_{ei}y_{oi}=1, \qquad \text{for } i=1,2,\cdots,n \tag{1}$$

$$g_1(g_1+2g_2)=1. \tag{2}$$

Fig. 3 shows reflected and transmitted waves at a discontinuity interface and its equivalent signal flow graph. The reflection coefficient r and transmission coefficient t at the discontinuity interface are defined as

$$r=\frac{b}{a}=\frac{y_a-y_b}{y_a+y_b} \tag{3}$$

$$t=\frac{c}{a}=\frac{2\sqrt{y_a y_b}}{y_a+y_b} \tag{4}$$

where y_a and y_b are the normalized characteristic admittances, and $|a|^2$, $|b|^2$, and $|c|^2$ denote the incident power from the left, its reflected power and its transmitted power,

0018-9480/81/0200-0118$00.75 ©1981 IEEE

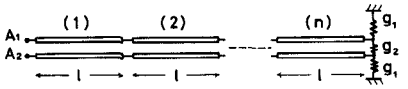

Fig. 1. A constant-resistance coupled-line network of n-section.

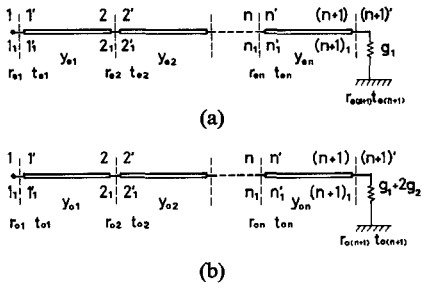

Fig. 2. Equivalent circuits. (a) Even mode. (b) Odd mode.

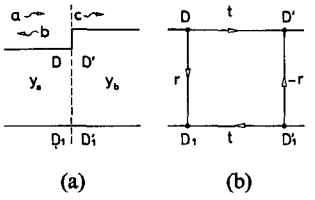

Fig. 3. (a) Reflected and transmitted waves at a discontinuity interface. (b) Its equivalent signal flow graph, where both incident waves from the left and from the right are considered.

respectively. From $|c|^2=|a|^2-|b|^2$

$$t^2=1-r^2. \tag{5}$$

Using (1) and (2), the reflection and transmission coefficients of the equivalent circuit shown in Fig. 2 are given by

$$r_{ej}=-r_{oj}=\frac{y_{e(j-1)}-y_{ej}}{y_{e(j-1)}+y_{ej}}, \qquad \text{for } j=2,3,\cdots,n \tag{6a}$$

$$r_{e1}=-r_{o1}=(1-y_{e1})/(1+y_{e1}) \tag{6b}$$

$$r_{e(n+1)}=-r_{o(n+1)}=(y_{en}-g_1)/(y_{en}+g_1) \tag{6c}$$

$$t_{ej}=t_{oj}=\frac{2\sqrt{y_{e(j-1)}y_{ej}}}{y_{e(j-1)}+y_{ej}}, \qquad \text{for } j=2,3,\cdots,n \tag{7a}$$

$$t_{e1}=t_{o1}=2\sqrt{y_{e1}}\,/(1+y_{e1}) \tag{7b}$$

$$t_{e(n+1)}=t_{o(n+1)}=2\sqrt{y_{en}g_1}\,/(y_{en}+g_1) \tag{7c}$$

where $t_{ej}^2=1-r_{ej}^2$, $j=1,2,\cdots,n+1$. Since each equivalent circuit for even and odd modes shown in Fig. 2 has $(n+1)$ discontinuity interfaces and n commensurate lossless transmission-line sections, an equivalent signal flow graph for each mode can be obtained by having the commensurate transmission-line sections looked on as delay operators and replacing the discontinuity interfaces with the signal flow graph as shown in Fig. 3(b). Fig. 4 shows

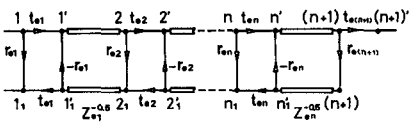

Fig. 4. A signal flow graph representation of the even-mode equivalent circuit.

the resultant signal flow graph for the even mode except for the terminated conductance g_1. Let the delay operators for the even and odd modes be z_{ei} and z_{oi} $(i=1,2,\cdots,n)$, respectively. For the homogeneous dielectric medium of the coupled line, $z=z_{ei}=z_{oi}$. Since z^{-1} is equal to transfer function of lossless one-strip transmission-line having line length $2l$, it can be written as

$$z^{-1}=e^{-2j\beta l}=e^{-2s\tau} \tag{8}$$

where $s=j\omega$, β is a phase constant, and τ is a time delay for the line length l. However, for the nonhomogeneous medium, $z_{ei}\neq z_{oi}$, $z_{ei}\neq z_{ek}$, and $z_{oi}\neq z_{ok}$ $(i=1,2,\cdots,n;\ k=1,2,\cdots,n;\ i\neq k)$. A signal flow graph representation for odd mode is simply given by replacing r_{ej}, t_{ej}, and z_{ei} with r_{oj}, t_{oj}, and z_{oi} in Fig. 4.

When an incident impulse $\delta(t)/2$ is applied to each port 1 of these even- and odd-mode signal flow graphs, let the each output response obtained from each port 1_1 be $b_{en}(t)$ and $b_{on}(t)$. Consider the true voltage responses $v_1(t)$ and $v_2(t)$ at port A_1 and A_2 shown in Fig. 1 [14]. Assuming the incident impulses $\delta(t)/2$, $\delta(t)/2$ for port A_1 and incident impulses $\delta(t)/2$, $-\delta(t)/2$ for port A_2 are simultaneously applied, then the $v_1(t)$ and $v_2(t)$ can be given as

$$v_1(t)=\delta(t)+b_{en}(t)+b_{on}(t) \tag{9}$$

$$v_2(t)=b_{en}(t)-b_{on}(t) \tag{10}$$

because the normalized impedances connected with port A_1 and A_2 are unity. Here, $\delta(t)$ is the Dirac delta function. In the case of homogeneous coupled line, $b_{en}(t)$ and $b_{on}(t)$ are given by [6]

$$b_{en}(t)=\sum_{k=0}^{\infty} g_{ek}\delta(t-2k\tau) \tag{11}$$

$$b_{on}(t)=\sum_{k=0}^{\infty} g_{ok}\delta(t-2k\tau) \tag{12}$$

where g_{ek} and g_{ok} are the amplitudes of the returning waves for the even and odd modes at port 1_1 at $t=2k\tau$. A close inspection gives that g_{ek} is composed of the product of even number of transmission coefficients and odd number of reflection coefficients. This is also the same as g_{ok}. From (6) and (7), $g_{ek}=-g_{ok}$. Thus

$$v_1(t)=\delta(t) \tag{13}$$

$$v_2(t)=2b_{en}(t). \tag{14}$$

Therefore, there are no reflected waves at port A_1, and output response at port A_2 for an incident unit impulse at port A_1 can be analyzed by using only signal flow graph of even mode. When $t_{ej}^2=1-r_{ej}^2$, by the use of mathematical

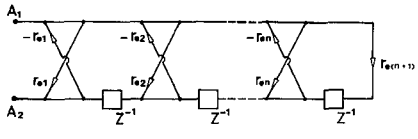

Fig. 5. The equivalent signal flow graph with lattice structures.

induction, we can substantiate that Fig. 4 is equivalent to Fig. 5 having lattice structures.

III. Output Waveforms of the Constant-Resistance Coupled-Line Network for Periodic Square Pulse Inputs

Let the duration t_1 of incident periodic pulse be less than 2τ, for the successive output pulses will not overlap. If the normalized characteristic admittances for the even and odd modes of two-strip coupled line of single section are y_{0e} and y_{0o}, the coupling coefficient k and the coupling K dB to the adjacent stripline are defined as [15]

$$k=(y_{0o}-y_{0e})/(y_{0o}+y_{0e}) \tag{15}$$

$$K=-10\log_{10}k^2. \tag{16}$$

A. In the Case of Microwave C-Type Section of Single Section

A microwave C-type section of single section can be obtained from Fig. 1 for $g_1=0$ and $n=1$ [3]. Its transient responses are shown in Fig. 6. The sum of output voltages of even number, $S_{et}=\sum_{i=1}^{\infty}v_{2i}$ converges to unity and the sum of output voltages of odd number, $S_{ot}=\sum_{i=1}^{\infty}v_{2i-1}$ converges to zero. From Fig. 6(c), the microwave C-type section in stationary state can be considered as a delay line which delays incident square pulse with period 4τ for 2τ.

B. In the Case of Constant-Resistance Coupled-Line Network of Single Section

Consider the periodic square pulse with period 4τ shown in Fig. 6(a) as an incident pulsetrain, then the pulses of even number in transient response derived from a single pulse are superimposed and the pulses of odd number are similarly superimposed. Let the sum of even pulses and the sum of odd pulses be S_{et} and S_{ot} in the same manner as above mentioned A:

$$S_{et}=\frac{(y_{e1}+g_1)(y_{e1}-g_1)}{(1+g_1)(g_1+y_{e1}^2)} \tag{17}$$

$$S_{ot}=\frac{g_1(1-y_{e1}^2)}{(1+g_1)(g_1+y_{e1}^2)} \tag{18}$$

where g_1 is variable parameter on a restriction of (2) and y_{e1} is determined by (16). Four cases of $g_1=0, y_{e1}^2, y_{e1}$, and 1 are stated as follows.

1) For $g_1=0$, $S_{ot}=0$, $S_{et}=1$. This is the case of microwave C-type section.

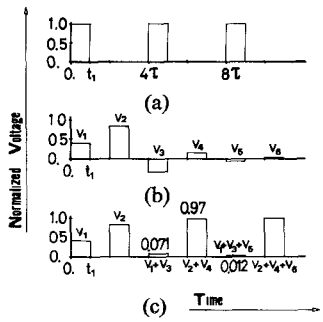

Fig. 6. Input and output voltage waveforms of a microwave C-section of single section having 3-dB coupling. (a) Input unit square pulsetrain with period 4τ and duration t_1. (b) Transient response for a unit single square pulse. (c) Transient response for the pulsetrain of (a).

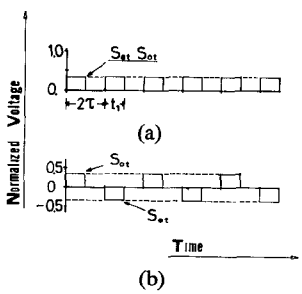

Fig. 7. Output voltage waveforms of the treated network of single section for unit pulse train shown in Fig. 6(a). (a)$g_1=y_{e1}^2$. (b) $g_1=1$.

2) For $g_1=y_{e1}^2$

$$S_{ot}=S_{et}=0.5(1-g_1)/(1+g_1) \tag{19}$$

which means that output pulsetrain with period 2τ whose amplitude is less than 0.5 can be obtained from the incident unit pulse train with period 4τ. Thus, the coupled-line network can be considered as a digital frequency doubler consisting of passive elements.

3) For $g_1=y_{e1}$, S_{ot} takes the maximum value and r_{e2} is equal to zero. Therefore, the coupled-line network does not produce any transient responses for a single pulse, and makes only the amplitude of incident pulsetrain smaller.

4) For $g_1=1$, $S_{ot}=-S_{et}=0.5(1-y_{e1}^2)/(1+y_{e1}^2)$. The coupled-line network is so called as a directional coupler [16].

The cases of 2) and 4) are depicted in Fig. 7(a) and (b).

C. Digital Frequency Multiplier Consisting of Constant-Resistance Coupled-Line Network of Multisection

Subsequently, we consider the coupled-line network of multisection, because of expectation that digital frequency multiplier may be realized without active elements. The transfer function of the network shown in Fig. 1 is given by

$$\frac{b_n(z)}{a_n(z)}=\frac{a_0+a_1z^{-1}+a_2z^{-2}+\cdots+a_nz^{-n}}{1+b_1z^{-1}+b_2z^{-2}+\cdots+b_nz^{-n}} \tag{20}$$

where $b_n(z)$ and $a_n(z)$ refer to the output and input in z-domain. The incident impulse train with period $2(n+1)\tau$ is written in z-domain as

$$a_n(z)=1/\left[1-z^{-(n+1)}\right]. \tag{21}$$

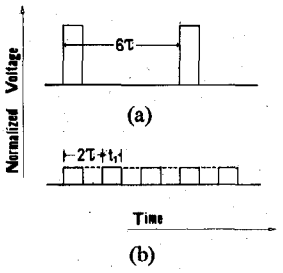

Fig. 8. Input and output pulsetrain of the proposed digital frequency tripler. (a) Input square pulsetrain. (b) Output square pulsetrain.

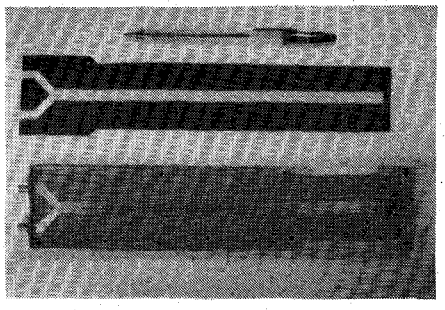

Fig. 9. A photograph of the proposed digital frequency doubler.

Multipling (20) by (21) under the condition of $a_0 = a_1 = \cdots = a_n$, the partial fraction expansion of $b_n(z)$ is

$$b_n(z) = \frac{a_0}{E_n}\left[\frac{b_0' + b_1' z^{-1} + \cdots + b_{n-1}' z^{-n+1}}{1 + b_1 z^{-1} + \cdots + b_n z^{-n}} + \frac{1}{1 - z^{-1}}\right] \tag{22}$$

where $a_0 = r_{e1}$, $E_n = 1 + \sum_{i=1}^{n} b_i$, $b_0' = \sum_{i=1}^{n} b_i$, $b_1' = \sum_{i=2}^{n} b_i, \cdots$, and $b_{n-1}' = b_n$. The impulse response of the first term of $b_n(z)$ vanishes and only that of the second term remains in stationary state, because the denominator of the first term is equal to that of (20). The resultant waveform of (22) reveals an impulse train with period 2τ and amplitude a_0/E_n.

In the case of $n=2$, using Fig. 5, the transfer function is given by

$$\frac{b_2(z)}{a_2(z)} = \frac{r_{e1} + r_{e2}(1 + r_{e1}r_{e3})z^{-1} + r_{e3}z^{-2}}{1 + r_{e2}(r_{e1} + r_{e3})z^{-1} + r_{e1}r_{e3}z^{-2}}. \tag{23}$$

The incident unit impulse train with period 6τ is

$$a_2(z) = 1/(1 - z^{-3}). \tag{24}$$

Putting $r_{e1} = r_{e2}(1 + r_{e1}r_{e3}) = r_{e3}$ and multipling (23) by (24)

$$b_2(z) = \frac{r_{e1}}{E_2}\left[\frac{(2r_{e1}r_{e2} + r_{e1}^2) + r_{e1}^2 z^{-1}}{1 + 2r_{e1}r_{e2}z^{-1} + r_{e1}^2 z^{-2}} + \frac{1}{1 - z^{-1}}\right] \tag{25}$$

where $E_2 = 1 + 2r_{e1}r_{e2} + r_{e1}^2$. The inverse z-transform shows an impulse train with period 2τ and amplitude r_{e1}/E_2 in stationary state. If r_{e1} is known, $r_{e2} = r_{e1}/(1 + r_{e1}^2)$. The value of r_{e2} exists in a range of 0 to 1. Therefore, the r_{e2} satisfies the realizability condition with respect to reflection coefficients of the coupled-line network. Fig. 8 shows the input and output pulsetrains of a digital frequency tripler. In the case of $n=3$, following relations are obtained:

$$r_{e1} = r_{e4} \qquad r_{e2} = r_{e3} \tag{26a}$$

$$r_{e1}r_{e2}^2 + (1 + r_{e1}^2)r_{e2} - r_{e1} = 0. \tag{26b}$$

If r_{e1} is known, the quadratic equation (26b) has a root satisfying $0 < r_{e2} < 1$. Thus, the digital frequency four-time multiplier is obtained. In the case of $n=4$, numerical calculation of a cubic equation of the reflection coefficients has shown that the digital frequency five-time multiplier can also be realized.

In general, the realization scheme is to make the coefficients of numerator polynomial of (20) equal as $a_0 = a_1 = \cdots = a_n$, but the physical realizability conditions, i.e., $0 < r_{e1} < 1$, $r_{ej}^2 < 1$, for $j = 2, 3, \cdots, n$ and $r_{e(n+1)}^2 \leqslant 1$ must be tested for each element number.

IV. Experimental Results for Digital Frequency Doubler

In the previous sections, the incident pulsetrain is limited to square wave, but arbitrary input waveforms are available by the help of the convolution theorem and impulse response of the treated network. Fig. 9 shows a photograph of an experimental digital frequency doubler consisting of homogeneous coupled line network of single section. The top is a ball point pen, the second is a photomask for the photoetching, and the third one is an actual digital frequency doubler which was built without using active or nonlinear circuit elements. The input and output ports appear in the left side of the coupled line, and the three resistors of Π-structure are installed between the right end of the coupled line and the ground. These resistors were fabricated by thin films of Fe–Cr–Ti–Al system produced by radio frequency reactive sputtering [17], [18]. The dimensions of the coupled line depend on its coupling [19], and the values of the normalized conductances g_1 and g_2 are also given by the coupling through the relation of $g_1 = y_{e1}^2$, and (1), (2), (15), and (16). The design data of the experimental digital frequency doubler are as follows: $s = 0.12$ mm, $w = 3.94$ mm, $b = 8$ mm, $l = 240$ mm, $K = 6.95$ dB, $\sqrt{\epsilon'}\, Z_{0e} = 130.8\ \Omega$, $\sqrt{\epsilon'}\, Z_{0o} = 49.7\ \Omega$, $R_1 = 50/g_1 = 131.6\ \Omega$, $R_2 = 50/g_2 = 44.4\ \Omega$, $\epsilon' = 2.6$, and $S_{et} = 0.225$, where the s, w, and b represent the same notation with the ones that have been illustrated in Fig. 3(a) of literature [19], l is the coupled-line length, K is the coupling in decibles, ϵ' is the relative permittivity, Z_{0e} and Z_{0o} are the even- and odd-mode characteristic impedances, respectively, R_1 and R_2 are resistances corresponding to g_1 and g_2, respectively, and S_{et} is a theoretical amplitude of output pulse train to the unit input pulsetrain.

Fig. 10 shows the observed input and output voltage waveforms, and their peak-to-peak values are about 820 mV and 185 mV, respectively. The ratio of both values 0.226 indicates an excellent agreement with theoretical value 0.225. The time lag from the top to the next top of

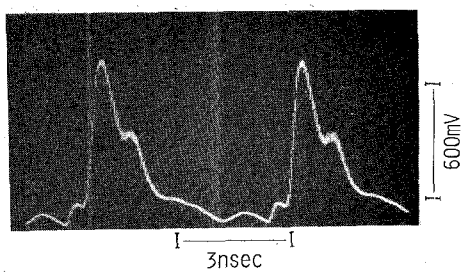

(a)

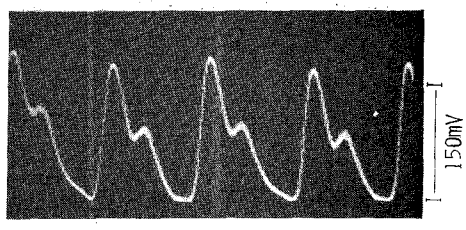

(b)

Fig. 10. Observed voltage waveforms of the proposed digital frequency doubler. (a) Input voltage waveform. (b) Output voltage waveform.

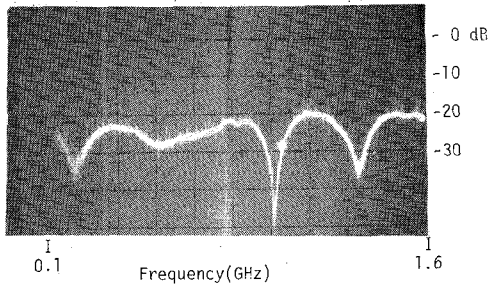

Fig. 11. Observed return loss of the proposed digital frequency doubler.

the waveforms shown in Fig. 10(a) is about 5.2 ns, which corresponds to clock frequency 192 MHz. If higher clock frequencies and transmission medium with higher relative permittivity than the experimental circuit are chosen, smaller circuits in size can be made.

Fig. 11 shows the observed return loss in decibels which is given by a ratio of reflected power to incident power at the input port. It is less than -20 dB or VSWR < 1.22 over the frequency range of 100 MHz to 1600 MHz. This means very good matching at the input port.

V. Conclusion

This paper has shown digital frequency multipliers such as doubler, tripler, and so on for input clock frequency can be designed without any active elements by using cascaded multisection of two-strip coupled-transmission-line and three resistors. On the digital frequency doubler, very close agreement has been obtained between experiment and theory. The simplicity of construction and high-speed capability make these multipliers attractive.

References

[1] H. Ogawa, S. Iisaku, E. Maekawa, and M. Tamori, "Constant-resistance coupled-line type networks and their applications," *Trans. Inst. Electron. Commun. Eng. Jap.*, vol. 58-B, pp. 435–440, Sept. 1975.

[2] S. O. Scanlan and J. D. Rhodes, "Microwave allpass networks part-I," *IEEE Trans. Microwave Theory Tech.*, vol. 16, pp. 62–72, Feb. 1968.

[3] S. O. Scanlan and J. D. Rhodes, "Microwave allpass networks part-II," *IEEE Trans. Microwave Theory Tech.*, vol. 16, pp. 72–79, Feb. 1968.

[4] E. G. Cristal, "Analysis and exact synthesis of cascaded commensurate transmission-line C-section all-pass networks," *IEEE Trans. Microwave Theory Tech.*, vol. MTT-14, pp. 285–291, June 1966.

[5] R. Levy, "General synthesis of asymmetric multi-element coupled-transmission-line directional couplers," *IEEE Trans. Microwave Theory Tech.*, vol. MTT-11, pp. 226–237, July 1963.

[6] G. F. Ross, "The transient analysis of certain TEM mode four-port networks," *IEEE Trans. Microwave Theory Tech.*, vol. MTT-14, pp. 528–542, Nov. 1966.

[7] W. J. Getsinger, "Analysis of certain transmission-line networks in the time domain," *IRE Trans. Microwave Theory Tech.*, vol. MTT-8, pp. 301–309, May 1960.

[8] K. A. Boakye and O. Wing, "On the analysis and realization of cascaded transmission-line networks in the time domain," *IEEE Trans. Circuit Theory*, vol. CT-20, pp. 301–307, May 1973.

[9] B. G. Bosch, "Gigabit electronics-A review," *Proc. IEEE*, vol. 67, pp. 340–379, Mar. 1979.

[10] L. J. P. Linner, "Time domain analysis of commensurate distributed-line networks," *IEEE Trans. Circuit and Systems*, vol. CAS-22, pp. 334–343, Apr. 1975.

[11] M. V. Schneider and W. W. Snell, Jr., "A scaled hybrid integrated multiplier from 10 to 30 GHz," *Bell Syst. Tech. J.*, vol. 50, pp. 1933–1942, July–Aug. 1971.

[12] K. W. Current and A. B. Current, "Frequency-doubling circuits for analogue and digital systems," *Int. J. Electron.*, vol. 45, pp. 431–441, 1978.

[13] T. Takeda and M. Hirayama, "Hybrid integrated frequency multipliers at 300 and 450 GHz," *IEEE Trans. Microwave Theory Tech.*, vol. MTT-26, pp. 733–737, Oct. 1978.

[14] H. J. Carlin and A. B. Giordano, *Network Theory: An introduction to Reciprocal and Nonreciprocal Circuits*. Englewood Cliffs, NJ,: Prentice-Hall, 1964.

[15] R. Levy, "Transmission-line directional couplers for very broad-band operation," *Proc. Inst. Elec. Eng.*, vol. 112, pp. 469–476, Mar. 1965.

[16] W. E. Caswell and R. F. Schwartz, "The directional coupler-1966," *IEEE Trans. Microwave Theory Tech.*, vol. MTT-15, pp. 120–123, Feb. 1967.

[17] T. Umezama and S. Yajima, "On the cermet thin films of Ni–Ta–Al–N system produced by radio frequency reactive sputtering," *Trans. Inst. Electron. Commun. Eng. Jap.*, vol. 58-C, pp. 266–273, May 1975.

[18] T. Umezawa and S. Yajima, "Electrical properties of dielectric thin films of the tantalum oxide-quartz system prepared by R. F. reactive sputtering," *Thin Solid Films*, vol. 29, pp. 43–52, 1975.

[19] S. B. Cohn, "Shielded coupled-strip transmission line," *IRE Trans. Microwave Theory Tech.*, vol. MTT-3, pp. 29–38, Oct. 1955.